

THE OFFICIAL MAGAZINE OF THE OCEANOGRAPHY SOCIETY

Oceanography

CITATION

Allard, R., E. Rogers, P. Martin, T. Jensen, P. Chu, T. Campbell, J. Dykes, T. Smith, J. Choi, and U. Gravois. 2014. The US Navy coupled ocean-wave prediction system. *Oceanography* 27(3):92–103, <http://dx.doi.org/10.5670/oceanog.2014.71>.

DOI

<http://dx.doi.org/10.5670/oceanog.2014.71>

COPYRIGHT

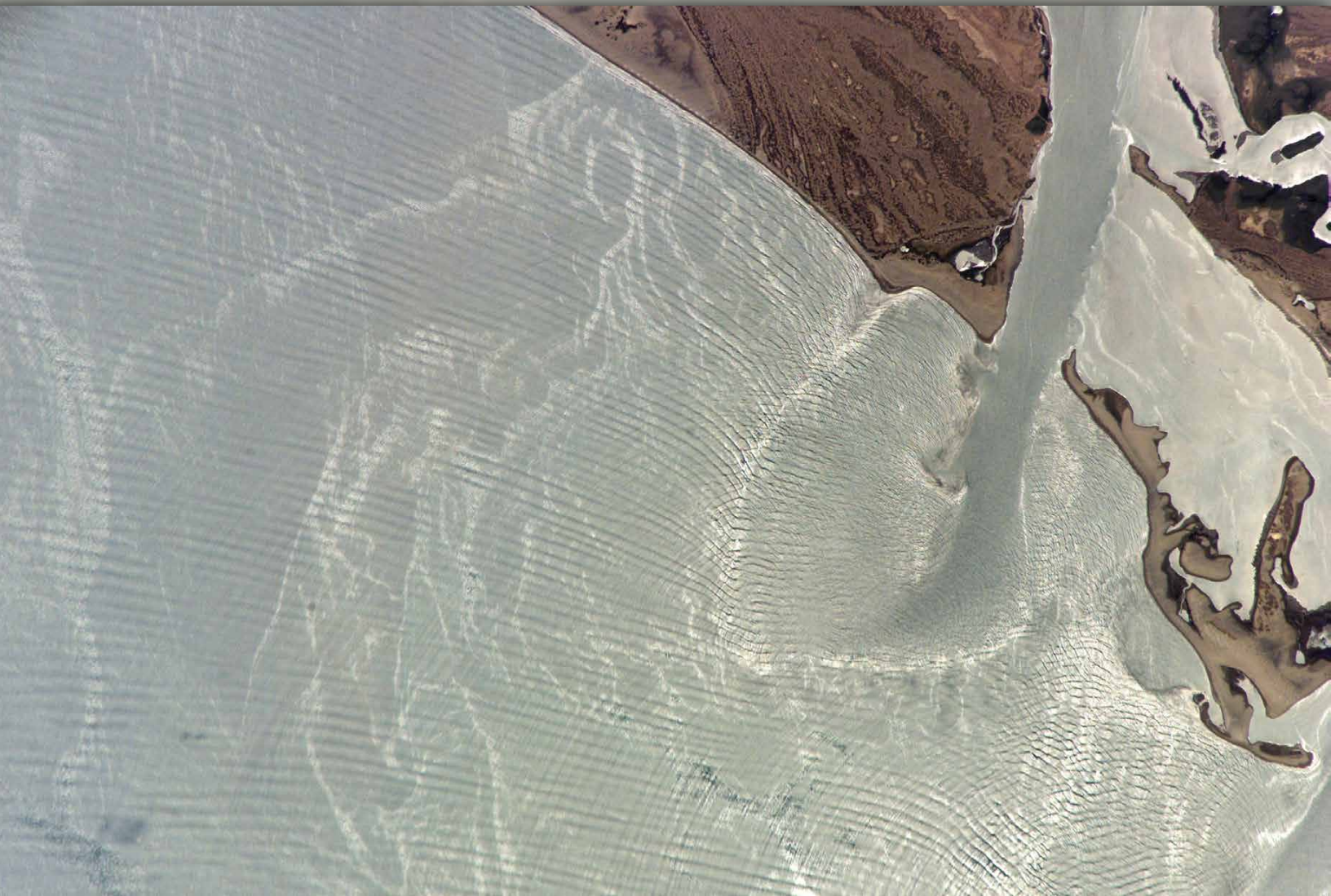
This article has been published in *Oceanography*, Volume 27, Number 3, a quarterly journal of The Oceanography Society. Copyright 2014 by The Oceanography Society. All rights reserved.

USAGE

Permission is granted to copy this article for use in teaching and research. Republication, systematic reproduction, or collective redistribution of any portion of this article by photocopy machine, reposting, or other means is permitted only with the approval of The Oceanography Society. Send all correspondence to: info@tos.org or The Oceanography Society, PO Box 1931, Rockville, MD 20849-1931, USA.

The US Navy Coupled Ocean-Wave Prediction System

BY RICHARD ALLARD, ERICK ROGERS, PAUL MARTIN,
TOMMY JENSEN, PHILIP CHU, TIM CAMPBELL, JAMES DYKES,
TRAVIS SMITH, JEIKOOK CHOI, AND URIAH GRAVOIS



NASA image taken May 9, 2006, from the International Space Station, showing the outgoing tidal current and complex wave patterns near Punta Perihuate, Mexico, on the eastern shore of the Gulf of California south of Los Mochis. Image credit: Science and Analysis Laboratory, NASA-Johnson Space Center. "The Gateway to Astronaut Photography of Earth." <http://eol.jsc.nasa.gov/scripts/sseop/photo.pl?mission=ISS013&roll=E&frame=16599>12/14/2013 18:18:11>

ABSTRACT. A new coupled ocean-wave model has been developed and tested as a new component of the Coupled Ocean/Atmosphere Mesoscale Prediction System (COAMPS®). The modeling system is comprised of the Simulating WAVes Nearshore (SWAN) wave model and the Navy Coastal Ocean Model (NCOM). The models are two-way coupled using the Earth System Modeling Framework (ESMF). The ocean model has been modified to incorporate the effect of the Stokes drift current, wave radiation stresses due to horizontal gradients of the momentum flux of surface waves, enhancement of bottom drag in shallow water, and enhanced vertical mixing due to Langmuir turbulence. The wave model ingests surface currents (wave-current interaction) and water levels. The system is designed to support the Navy's ocean forecast requirements for regional and coastal domains. Validation studies for the Florida Straits and Virginia coastal area are presented. The system will run at the Naval Oceanographic Office and at the Fleet Numerical Meteorology and Oceanography Center.

INTRODUCTION

The operational Navy requires accurate ocean and wave predictions to support search and rescue, anti-piracy initiatives, route planning, mine warfare, anti-submarine warfare, and amphibious operations. This information is also used as input to tactical decision aids such as mission planning tools to determine the optimal placement of sensors capable of collecting valuable information about ocean state. Furthermore, accurate forecasts are important for the prediction of the dispersion of contaminants as well as the projected path of a drifting mine field.

Several regional modeling systems developed over the past decade address ocean-wave coupling for numerous applications. The Delft3D modeling system (Lesser et al., 2004) couples the hydrodynamic FLOW model with the Simulating WAVes Nearshore (SWAN) model. Warner et al. (2008) coupled SWAN to the Regional Ocean Modeling System (ROMS) in which the Model-Coupling Toolkit is used to exchange wave and ocean circulation information between the model components. In both of these examples, the coupled ocean-wave modeling system is used to

drive sediment transport models. Tang et al. (2007) studied the impact of surface waves on Grand Banks surface currents using a coupled current-wave drifter model. Their analysis showed the Stokes drift to be the dominant wave effect and that it increased surface drift speeds by 35% and veered the current in the direction of the wind. Qiao et al. (2010) studied the impact of surface waves on the general ocean circulation by coupling the Princeton Ocean Model (POM) to a spectral wave model, and they found significant improvements in the upper mixed layer and seasonal thermocline by including wave-induced mixing. Singhal et al. (2013) examined the impact of ocean-wave coupling in Cook Inlet, Alaska, with the SWAN model coupled to a three-dimensional circulation model. They examined a 12-day period in October 2008 that included four significant storm events by performing one- and two-way coupling studies. Singhal et al. (2013) found that inclusion of currents in the wave model increased the significant wave heights by as much as 0.5 m, but saw marginal impact on the currents when waves were included. They concluded that accurate wind forcing was critical in obtaining an accurate forecast.

The coupled ocean-wave component described in this paper is part of the Coupled Ocean/Atmosphere Mesoscale Prediction System (COAMPS®). Descriptions of the atmospheric component of COAMPS can be found in Hodur (1997) and Doyle (2002). COAMPS supports the operational Navy with short-term (0–96 hour) forecasts for numerous regions throughout the globe. In addition, Doyle et al. (2014, in this issue) describe the tropical cyclone version of the system (COAMPS-TC). Existing (uncoupled) atmospheric forcing fields from COAMPS drive the coupled ocean-wave prediction system. The system does support a fully coupled atmosphere-ocean-wave capability, which is targeted for operational implementation in 2015. Figure 1 depicts an example of ocean temperature and currents derived from the ocean-wave system for the Chesapeake Bay area.

This paper provides an overview of the ocean and wave model components, coupling strategy, data assimilation, and initial/boundary conditions required for the system. Validation studies performed in the Florida Straits and along the Virginia Coast are presented to assess model skill.

NAVY COASTAL OCEAN MODEL OVERVIEW

The Navy Coastal Ocean Model (NCOM) was initially developed at the Naval Research Laboratory (NRL) in the 1990s for coastal ocean modeling (Martin, 2000). It provided high vertical resolution through vertical coordinate as well as multiple mixing parameterizations. NCOM was subsequently modified to couple within the same program as the atmospheric component of COAMPS. The requirement for multiple, coupled ocean nests to be run within

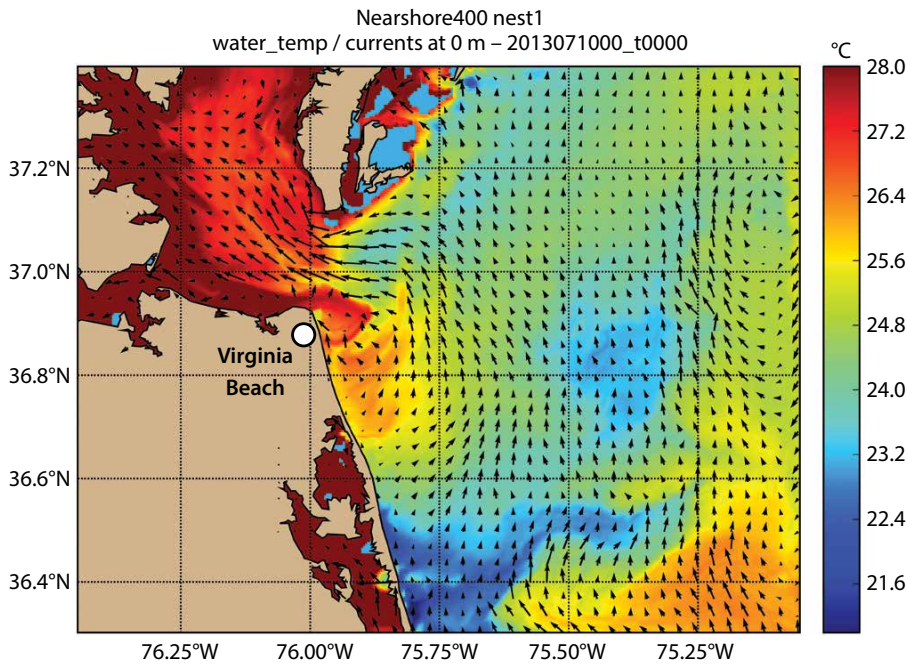


Figure 1. Model of sea surface temperature (°C) and ocean surface currents near the mouth of Chesapeake Bay on July 10, 2013. The model result is from a coupled ocean-wave prediction with a horizontal resolution of 400 m.

the same program determined NCOM's basic architecture.

As noted by Martin (2000), the basic physics and numerics of NCOM are similar to those of the POM (Blumberg and Mellor, 1987), but with a few differences. Like POM, NCOM assumes a hydrostatic, incompressible fluid that is Boussinesq and has a free surface. A curvilinear grid is used in the horizontal to allow the use of various map projections and some degree of grid curvature (Blumberg and Herring, 1987).

The original vertical grid uses a combination of sigma coordinates in the upper ocean and, optionally, fixed-depth coordinates from a user-specified depth

to the bottom. This combination permits the use of bottom-following sigma coordinates in shallow water (on the shelf, for example) and fixed-depth coordinates in deeper water, which can help reduce sigma-coordinate problems in cases of steep slopes (Haney, 1991). NCOM currently also allows the use of generalized sigma coordinates, either in the upper ocean or throughout the water column, where the fractional thicknesses of the layers can vary horizontally as well as vertically, and the number of sigma layers can be reduced as the water shallows. This allows a wide variety of vertical grids (e.g., Dukhovskoy et al., 2009).

Like POM, NCOM uses an Arakawa C

grid, with the velocity components centered on the faces of the main grid cells. The temporal scheme is leapfrog, with an Asselin filter to suppress time splitting (Asselin, 1972). The default spatial finite differences are mostly second order. There are options for third-order upwind (Holland et al., 1998) and fourth-order advection, and there are options for fourth-order differences for horizontal baroclinic pressure gradients and for interpolation of Coriolis terms. There is an option to use the Flux-Corrected Transport (FCT) scheme (Zalesak 1979) for advection of scalar fields, which prevents advective overshoots.

The free-surface mode is computed implicitly. Temporal weightings to be used for old, current, and new time levels for horizontal transports in the depth-averaged continuity equation and for the surface pressure gradient in the depth-averaged momentum equations can be set by the user; the default is an even split between the old and new time levels.

For horizontal mixing, NCOM offers the choice of a grid-cell Reynolds number scheme (Dietrich and Ko, 1994), the Smagorinsky (1963) scheme, or biharmonic mixing scaled by the advection velocity, which is part of the third-order upwind advection scheme (Holland et al., 1998). For vertical mixing, there is a choice of the Mellor-Yamada Level 2 (Mellor and Yamada, 1974; Mellor and Durbin, 1975) or Level 2.5 (Mellor and Yamada, 1982) turbulence schemes.

NCOM was run as a global, operational ocean forecast model at the Naval Oceanographic Office (NAVOCEANO) from 2006 to 2013 (Barron et al., 2004), and it is currently being run at NAVOCEANO as a regional forecast model in a number of areas described by Rowley et al. (2014, in this issue).

Richard Allard (*richard.allard@nrlssc.navy.mil*) is Oceanographer, **Erick Rogers** is Oceanographer, **Paul Martin** is Oceanographer, **Tommy Jensen** is Oceanographer, **Philip Chu** is Oceanographer, **Tim Campbell** is Oceanographer, **James Dykes** is Physical Scientist, and **Travis Smith** is Oceanographer, all at the Naval Research Laboratory, Stennis Space Center, MS, USA. **Jeikook Choi** is Oceanographer, Naval Oceanographic Office, Stennis Space Center, MS, USA. **Uriah Gravois** is a PhD candidate at the University of Florida, Gainesville, FL, USA.

NCOM is run at NRL as a stand-alone ocean model, usually using archived atmospheric fields for surface forcing, or as part of the COAMPS coupled atmosphere-ocean-wave system. This paper addresses ocean-wave coupling in COAMPS.

SWAN OVERVIEW

The wave model component of COAMPS is SWAN (Booij et al., 1999; SWAN Team, 2010), a model designed to run efficiently at high resolutions (e.g., 2 km or finer) through the use of implicit propagation methods. The numerical features of COAMPS SWAN are unchanged from standard SWAN (Booij et al., 1999). The default option for physics of COAMPS SWAN is to utilize wind input (S_{in}), whitecapping (S_{ds}), and non-breaking dissipation (S_{swell}) parameterizations, which are essentially those of Rogers et al. (2012), with minor updates. We provide the key features here, but refer the reader to Rogers et al. (2012) for details. The wind input term S_{in} is based on Donelan et al. (2006) and Tsagareli et al. (2010), developed from direct measurements of wind input at Lake George, Australia, with the wind drag coefficient based on Hwang (2011). Dissipation from breaking (whitecapping), S_{ds} , is based on Babanin et al. (2010), which is developed from Young and Babanin (2006), Tsagareli (2009), and Banner et al. (2000). S_{ds} is two phase—insofar as it accounts for breaking of waves due to inherent instability and dissipation induced by the breaking of longer waves—and employs a breaking threshold based on the Phillips (1958) saturation spectrum. Another dissipation, S_{swell} , included to account for the slow attenuation of swell by nonbreaking processes, utilizes work by Ardhuin et al. (2009,

2010). For four-wave nonlinear interactions, S_{nl4} , the default method of SWAN Team (2010), the Discrete Interaction Approximation, is used without modification.

OCEAN-WAVE COUPLING

The feedback of the ocean model to the wave model consists of the input of NCOM surface currents and water levels to SWAN. Water levels modify the water depth used within the wave model physics calculations, though this effect is only significant if the water depth is sufficiently shallow that the waves feel the bottom. More importantly, the surface currents input to the wave model alter the effective wind speed (i.e., the wind speed relative to a frame of reference moving with the currents), and the horizontal shear of the currents produces changes in the length, height, and direction of the waves in a manner similar to refraction and shoaling by interaction

nonconservative process.

The feedback of the wave model to the ocean model (i.e., SWAN to NCOM) includes the Stokes drift current (SDC) from the waves due to the wave motion, the wave radiation stress gradients, and the characteristic velocity and frequency of the wave orbital motion near the bottom. The wave motion near the bottom is used to enhance the bottom drag in shallow water using the parameterization described by Signell et al. (1990) and Davies and Lawrence (1994). The wave-radiation stress gradients from SWAN are applied in NCOM as a surface stress. The SDC from SWAN is included within the Coriolis term in NCOM's momentum equations (referred to as the Stokes-Coriolis term), is used to advect all the ocean model fields, and is included within NCOM's continuity equation (these SDC terms are implemented as in Bennis et al., 2011).

The SDC is also used in the param-

“ THE OPERATIONAL NAVY REQUIRES ACCURATE OCEAN AND WAVE PREDICTIONS TO SUPPORT SEARCH AND RESCUE, ANTI-PIRACY INITIATIVES, ROUTE PLANNING, MINE WARFARE, ANTI-SUBMARINE WARFARE, AND AMPHIBIOUS OPERATIONS. ”

with variable bathymetry. These are conservative processes; for example, shoaling is associated with conservation of the wave energy flux. However, this can, in turn, lead to nonconservative effects. For example, waves that become more (less) steep due to interaction with currents will be more (less) likely to break, and this breaking, also called whitecapping, is a highly nonlinear and

eterization of the enhancement of vertical mixing by Langmuir turbulence, as described by Kantha and Clayson (2004). Additional shear-production terms that consist of the product of the vertical shear of the SDC and the vertical turbulent momentum flux are added to the turbulent kinetic energy (TKE) and vertical turbulent length-scale (TLS) equations in the Mellor-Yamada

Level 2.5 turbulence model to compute the vertical mixing coefficients in NCOM (Martin et al., 2013). These additional shear-production terms are referred to as Stokes production terms. The effect of the implementation of the Kantha and Clayson parameterization of enhanced mixing by Langmuir turbulence in NCOM is to increase the rate of mixing in the surface mixed layer by a factor of two to three and to slightly increase the depth of mixing (Martin et al., 2013). See Allard et al. (2012) and Smith et al. (2013) for additional information on the ocean-wave coupling in COAMPS.

DESCRIPTION OF COUPLING SOFTWARE

The COAMPS software infrastructure for coupling is built upon the Earth System Modeling Framework (ESMF; <http://www.earthsystemmodeling.org>) together with the National Unified Operational Prediction Capability (NUOPC) interoperability software layer (<http://earthsystemcog.org/projects/nuopc>), which defines conventions and templates for using ESMF. The system (shown in Figure 2) consists of individual model components (atmosphere, ocean, wave), a coupling layer, and a driver. The model components interface with the

coupled system via an ESMF software layer implemented within each model. The model ESMF layer sets up a mapping between the model's internal data structures and the ESMF data structures that are used for intermodel data transfer. The model ESMF layer also implements methods (as defined by the NUOPC convention) that enable the driver to invoke the initialization, time stepping, and finalization phases of the model. Data exchange between the models, consisting of interpolation of fields from a source model grid to a destination model grid, is implemented in the coupling layer (depicted by arrows in Figure 2). During initialization, each model specifies the import fields it requires and the export fields it can provide. The coupling layer establishes the connections between the models by matching each import field of a "consumer" model with an export field of a "producer" model. The driver layer, the harness for the models and coupling, coordinates the allocation of resources, initialization, and time stepping of the models. Campbell et al. (2010) and Chen et al. (2010) describe additional implementation details. The ocean-wave coupling described in this manuscript does not include two-way coupling with the atmosphere.

BOUNDARY CONDITIONS

The ocean component of the coupled ocean-wave prediction system receives initial and boundary conditions (BC) from the Navy's 1/12° global Hybrid Coordinate Ocean Model (HYCOM), which is run operationally at NAVOCEANO (Bub et al., 2014, and Metzger et al., 2014, both in this issue). The hybrid coordinate in HYCOM (Bleck, 2002; Metzger et al., 2014, in this issue) is isopycnal in the open, stratified ocean but smoothly reverts to a terrain-following coordinate in shallow coastal regions, and to z-level coordinates in the mixed layer and/or in unstratified seas. The SWAN wave component receives BC from the global WAVEWATCH III® (denoted here as WW3; Tolman, 2009) model, which is run operationally by the Fleet Numerical Meteorology and Oceanography Center (FNMOC) and NAVOCEANO. The global nature of these models ensures that the ocean-wave prediction system can be applied to essentially any ocean region.

OCEAN DATA ASSIMILATION

NCOM can assimilate real-time ocean observational data such as remotely sensed sea surface temperature, sea surface height, in situ surface and subsurface observations of temperature and salinity, and measurements from ships, buoys, expendable thermographs, and floats using the Navy Coupled Ocean Data Assimilation (NCODA) system (Cummings, 2005). NCODA is a fully three-dimensional, multivariate, optimum-interpolation ocean data assimilation system. The system is run in real time and can be executed in a stand-alone analysis or can be run as part of an ocean forecast cycle. The operational SWAN model described in this paper

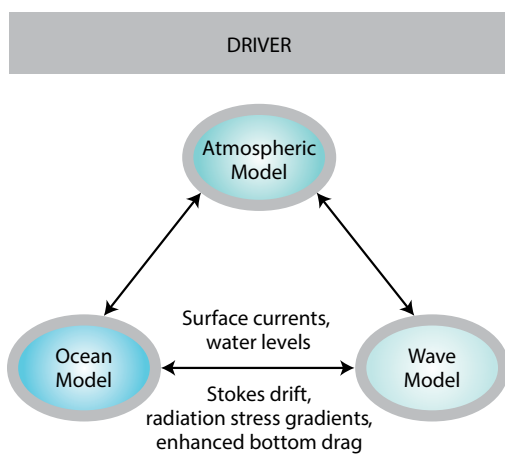


Figure 2. Schematic of Coupled Ocean/Atmosphere Mesoscale Prediction System (COAMPS®) software infrastructure. A software layer implemented within each model (gray band around each model) interfaces between the Earth System Modeling Framework (ESMF) and the model's internal methods and data structures. The coupling layer (arrows) handles the data exchange between the models using ESMF methods for parallel regridding and redistribution of data. The driver layer provides a harness for the models and the coupling, coordinating the allocation of resources, initialization, and time-stepping.

does not presently assimilate wave data; however, a SWAN wave adjoint capability described by Veeramony et al. (2014, in this issue) can assimilate directional wave spectral data. This new wave data assimilation with SWAN will be incorporated into a future version of COAMPS.

VALIDATION STUDIES

This section describes two applications of the two-way coupled ocean-wave prediction system: (1) the Florida Straits, and (2) the Virginia coast near the mouth of Chesapeake Bay.

Florida Straits Model Setup

Three wave model grids were used for this validation effort. WW3 is run on the outermost grid (wave grid 1, including the Atlantic Ocean at 0.5° resolution) with archived wind forcing from the Navy's Operational Global Atmospheric Prediction System (NOGAPS; Hogan and Rosmond, 1991) and Digital Bathymetry Data Base (DBDB2) bathymetry. Another run is made with WW3 on wave grid 2 using boundary conditions generated from wave grid 1. Wave grid 2 also employs DBDB2 bathymetry but is forced by COAMPS. This grid has 4' (~7 km) resolution and includes ocean points in the region of the southeastern United States. The SWAN wave model is run on wave grid 3 coupled with NCOM every six minutes. Wave grid 3 is forced at the boundaries with WW3 grid 2 outputs. Figure 3a depicts the three grids used for the wave computations. This discussion will focus on the innermost grid 3.

Three simulations were performed for grid 3. A control model simulation was run first with full coupling between ocean and waves, and second as a simulation with ocean to wave coupling disabled. The second simulation was

run to quantify the impact of the coupling. The third simulation was a fully coupled simulation with bottom friction increased by a factor of three; this simulation indicated that the validation results are fairly insensitive to bottom friction.

The period for the COAMPS model validation in the Florida Straits was from March 1 to May 18, 2005. A detailed description of the wave model setup can be found in the report of Gravois et al. (2012), which we denote as "GRJ" below.

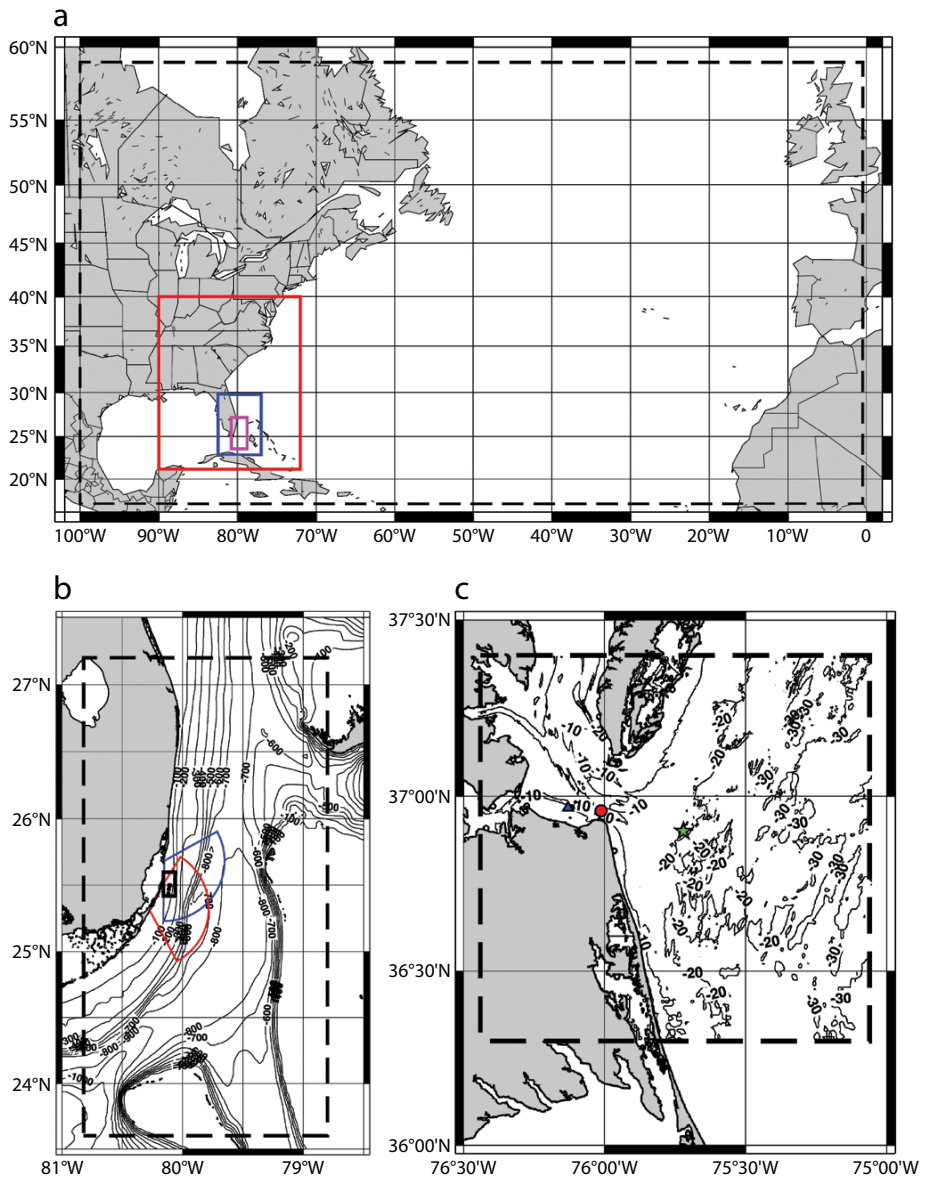


Figure 3. (a) Florida Straits model domain. The outer dashed black line represents WAVEWATCH III® (WW3) 55 km Nest 1. The red box denotes a WW3 7 km nest. The blue rectangle represents a 3 km Navy Coastal Ocean Model (NCOM) outer nest. The magenta box represents 1 km Simulating WAVes Nearshore (SWAN) wave model and NCOM inner nests. (b) Local bathymetry, in meters for grid 3 for a Florida Straits test case. The position of the two high-frequency Weller radar (WERA HF) stations located at Crandon Park (CDN; red) and North Key Largo Hammocks Biological Preserve (NKL; blue) are shown with swath wave sensing ranges. The small rectangular box in black includes the locations of the in situ data shown in Table 1. (c) Coupled NCOM-SWAN grid domain for Trident Warrior 2013 for coastal Virginia. The exercise is denoted by a black dashed line. Isobaths are shown at 10 m intervals. In situ measurements shown are from the NDBC Buoy 44099 (green star), the Cape Henry (red circle), and the Chesapeake Bay Bridge-Tunnel (blue triangle) National Ocean Service (NOS) stations.

Description of Validation Data

Ground truth for validation in this instance is from a combination of in situ and radar data. The in situ sensors (acoustic Doppler current profiler and buoy) provide robust and reliable wave and tide data with the disadvantage that they provide limited spatial coverage. The Rosenstiel School of Marine and Atmospheric Sciences (RSMAS) collected in situ data during the late spring/early summer of 2005. The instruments were positioned outside of Biscayne Bay, Miami, and recorded waves and currents at five point locations.

In addition to the in situ data, field measurements were also gathered by a pair of high-frequency Wellen radars (WERA HF) operated by RSMAS, described in Haus (2007), Haus et al. (2010), and Voulgaris et al. (2008). The two WERA HF radars located at Crandon Park (denoted “CDN,” 25°42.84'N, 80°9.06'W) on Key Biscayne and North Key Largo Hammocks Biological Preserve (denoted “NKL,” 25°14.46'N, 80°18.48'W) are separated by a distance of approximately 55 km. The spatial coverage of the wave height radar data extends roughly 50 km from

the radar stations and spans over a 120° field of view centered on the boresight angle. The radar field grid spacing is regular at 1.2 km, with 1,682 cells for the CDN radar and 1,816 for the NKL radar. The sampling rate is 20 minutes. Figure 3b shows the WERA HF wave measurement areas.

The benefit of the radar data is that it provides large spatial coverage and density. However, with the increase in spatial coverage comes a decrease in confidence of the accuracy of the measurements. To make best use of the WERA HF data records used for this validation effort required substantial temporal filtering of outlier points and subsequent spatial and temporal averaging. The radar data were obtained in uncalibrated form and are calibrated in GRJ using comparisons between the in situ data and nearby radar values. The radar data are then divided into sectors for comparison with the model wave heights collocated with the sectors. By subdividing the data into equal-area sectors, essentially organizing them by distance and azimuth angle, we are able to interpret the data in the context of data quality, which is expected to

depend on distance and azimuth. The calibration and sector averaging are described in detail in GRJ.

Model Validation Against In Situ Measurements

Wave height, direction, and peak period from the numerical model in situ locations were compared against the measured in situ data. Table 1 shows the tabulated statistics for the wave height comparisons for the period April 1, 2005, to May 15, 2005. Comparisons include cases with and without wave-ocean coupling. The model with full wave-ocean coupling has reduced bias and root mean square error (RMSE), and improved correlation (*r*-statistic). Correlations were slightly better at the tri-axis buoy (TAB) stations, which were in deeper water. Plotted time series and analysis corresponding to these statistics can be found in GRJ.

Two swell events were over-predicted by the wave model at the nearshore site (compared to the in situ data) but not further offshore (compared to the radar). Nearshore over-prediction is caused by the model’s difficulty in treating swells that travel from the NNE, almost parallel to the coastline; blocking and scattering of wave energy by the bathymetry prior to arrival at the in situ site is not well represented. This is believed to be associated with the directional information in the wave boundary forcing, either (a) small errors in direction that cause energy to pass through, which should be blocked/scattered, or (b) resolution error—the directional resolution of the forcing is 10°. Other than these two swell events, the waves are well predicted by the model. Another interesting finding is made in GRJ about the propagation of swell energy to the nearshore location. Only waves of specific incident direction

Table 1. Tabulated statistics for wave height comparisons, model vs. RSMAS in situ data. Instrument type is shown in parentheses in the first column.

	Bias	RMSE	r-statistic
C1 (RDI ADCP)	0.09	0.23	0.69
C1 – no currents	0.18	0.31	0.65
C3 (TAB N)	0.08	0.23	0.74
C3 – no currents	0.18	0.31	0.67
C4 (SONTEK ADP)	0.22	0.32	0.68
C4 – no currents	0.31	0.41	0.62
C7 (TAB S)	0.04	0.19	0.80
C7 – no currents	0.13	0.26	0.72
C8 (RDI ADCP)	0.13	0.23	0.73
C8 – no currents	0.22	0.32	0.67

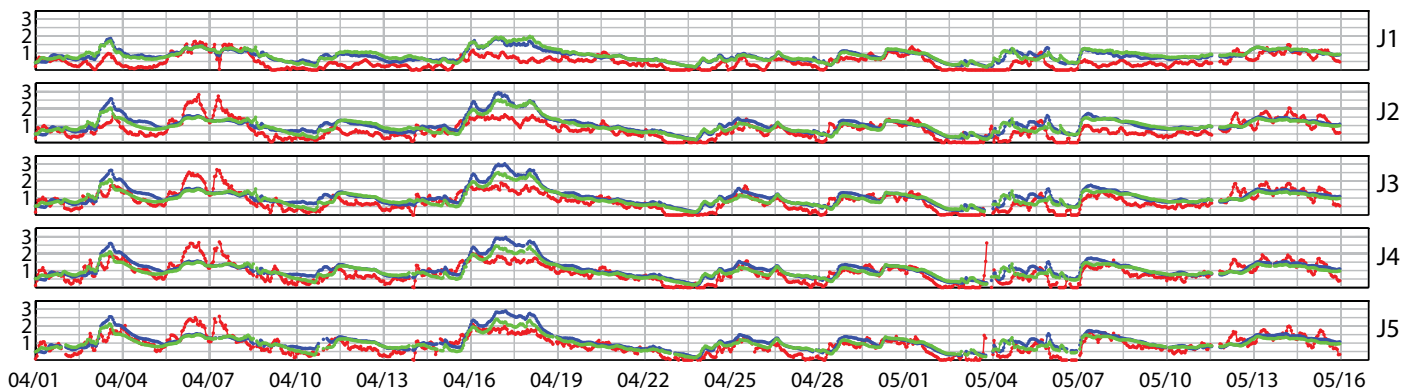


Figure 4. Example comparison of COAMPS (SWAN) fully coupled model output shown in blue vs. SWAN without currents (green) vs. calibrated radar (red). Significant wave height is in meters. The panels show results from section J at the KLN radar from nearshore J1 to offshore J5 (see Figure 5 for location of section).

are able to reach the nearshore location. This narrow aperture is found to be highly sensitive to the currents, which are directed NNE for the case with currents and NE for the case without currents. This is another argument for inclusion of currents in the modeling, though it is acknowledged that the wave boundary forcing must be of high fidelity to see this particular benefit. Otherwise, swell predictions will be poor, regardless, or even right for the wrong reasons. For additional information, the reader is referred to Figure 16 in GRJ and the related text.

Model Validation Against Radar

GRJ give time-series comparisons of the radar data against collocated model output. Figure 4 is an example plot. In this plot, and in similar plots not shown, the significant wave height of the “no currents” case (green line) is generally higher than the “with currents” case (blue line “control case”) in shallow water, while the reverse is true further offshore. This reinforces what is observed in the in situ vs. model comparisons: surface currents play a significant role in redirecting energy in the wave model. However, the mean bias for the larger wave events (April 4 and April 16) is

Table 2. The “r” correlation coefficient of model vs. WERA data sectors. Here, “nc” indicates wave model simulations performed without surface currents as input. Skill is for significant wave height, in meters. Statistics are calculated using the period April 1, 2005, to May 15, 2005. Black numbers indicate better correlation with full coupling. Red numbers indicate worse correlation with full coupling. Blue numbers indicate no difference.

		CDN Radar Site					NKL Radar Site						
		Increasing distance offshore →					Increasing distance offshore →						
		Nearshore		Offshore			Nearshore		Offshore				
		r@1	r@2	r@3	r@4	r@5	r@1	r@2	r@3	r@4	r@5		
NE azimuth	A	0.53	0.29	0.33	0.31	0.31	NE azimuth	G	0.26	0.52	0.61	0.58	0.67
	A_nc	0.51	0.24	0.31	0.29	0.29		G_nc	0.19	0.45	0.55	0.46	0.58
	B	0.67	0.72	0.63	0.65	0.67		H	0.65	0.66	0.72	0.74	0.75
	B_nc	0.64	0.67	0.57	0.63	0.65		H_nc	0.61	0.60	0.66	0.70	0.71
	C	0.47	0.70	0.73	0.73	0.73		I	0.64	0.65	0.68	0.70	0.72
	C_nc	0.49	0.69	0.69	0.71	0.71		I_nc	0.58	0.61	0.66	0.68	0.70
SE azimuth	D	0.28	0.77	0.79	0.81	0.81	J	0.63	0.63	0.70	0.71	0.75	
	D_nc	0.29	0.73	0.74	0.77	0.77	J_nc	0.59	0.63	0.70	0.72	0.75	
	E	0.36	0.71	0.81	0.80	0.79	SE azimuth	K	0.60	0.57	0.64	0.68	0.69
	E_nc	0.31	0.64	0.71	0.72	0.71		K_nc	0.56	0.58	0.66	0.69	0.71
	F	0.38	0.51	0.55	0.63	0.70		L	0.57	0.46	0.47	0.53	0.56
	F_nc	0.34	0.44	0.45	0.56	0.63		L_nc	0.52	0.46	0.49	0.55	0.58

positive. Because of this, the omission of surface currents in the wave forcing (green lines) actually results in a reduction in bias during these events. Because the positive background bias (discussed above) is unrelated to the surface currents, this is simply a cancellation of errors. To circumvent such spurious

effects, we focus primarily on correlation coefficients rather than on mean bias.

Table 2 provides the correlation coefficients from this comparison using HF radar as ground truth (bias and RMSE are provided in GRJ). In many cases, the inclusion of currents results in a modest improvement in the correlation score

and a decrease in the RMSE. Figure 5a,b shows the same statistics in graphical form. One worrisome feature is that the skill of the model is generally better near the center of the radar's boresight, with sections D, E, J, and K having relatively high correlation values. This suggests that model validation skill may have more to do with the quality (or lack thereof) of the observational data than the skill of the model to reproduce the spatial variability of the real ocean in the azimuthal position relative to the radar origin. However, comparisons such as those shown in Figure 4 indicate reasonably high prediction skill.

GRJ further find that another positive outcome from the comparison is that the spatial variability of the model in the context of the range position relative to the radar origin, roughly corresponding to the water depth, is also observed in the radar. The decrease in wave height toward shore is clearly seen in both the model and the radar, in excellent qualitative agreement.

Trident Warrior 2013 Exercise (Virginia Coast)

The ocean-wave modeling system in COAMPS was demonstrated during the Navy's annual Trident Warrior

Exercise in July 2013 off the Virginia coast. Trident Warrior demonstrates new and emerging technologies (White, 2013) and alternates US coasts every year (Trident Warrior 2014 will be based out of San Diego). A two-way coupled NCOM-SWAN grid was set up with 400 m grid resolution. High-resolution bathymetry was obtained from NOAA's Digital Elevation Model (Taylor et al., 2008). Boundary conditions for NCOM were provided by a host 1 km NCOM grid. Boundary conditions from WW3 were applied to the 400 m SWAN boundary. The operational Western Atlantic COAMPS 27 km regional grid provided atmospheric forcing. Tides were included in the NCOM model simulation with eight diurnal and semidiurnal tidal constituents (K1, O1, P1, Q1, K2, M2, N2, and S2). SWAN was run in stationary mode, which greatly reduced the run time of the model. SWAN and NCOM exchanged information at 12-minute intervals. Figure 3c depicts the 400 m ocean-wave domain, which extends from the mouth of Chesapeake Bay to approximately 80 km east of the northern Virginia coast.

Description of Validation Data

NDBC buoy 44099 is located 5 km ESE of Virginia Beach at 19 m water depth. Water level measurements were obtained for the Chesapeake Bay Bridge-Tunnel

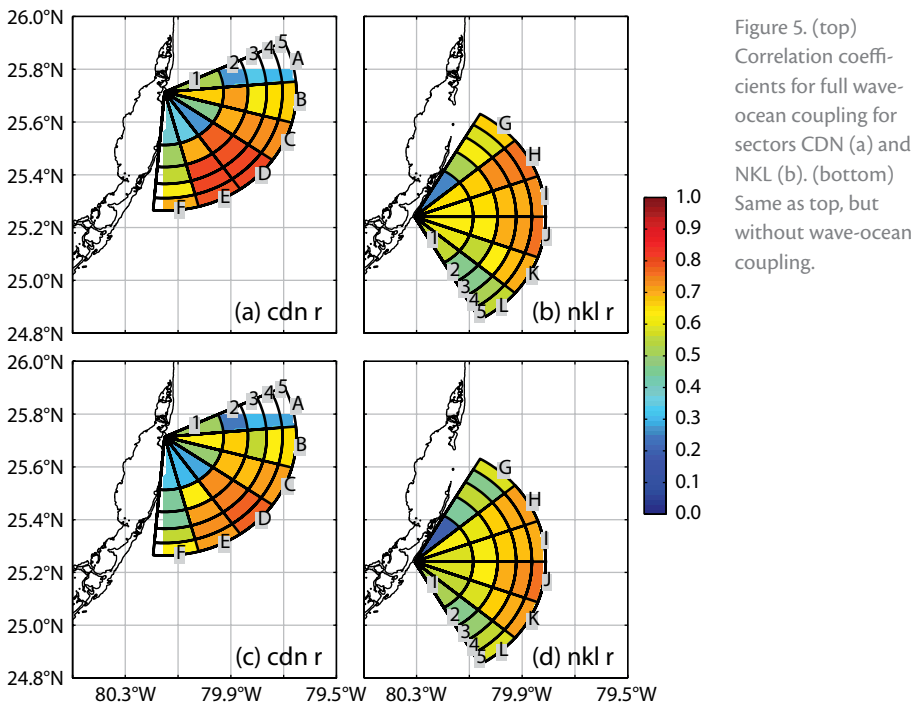


Figure 5. (top) Correlation coefficients for full wave-ocean coupling for sectors CDN (a) and NKL (b). (bottom) Same as top, but without wave-ocean coupling.

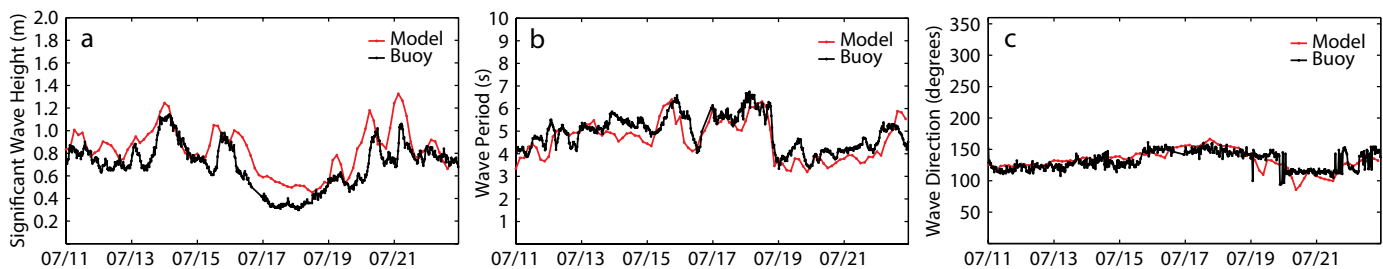


Figure 6. NDBC Buoy 44099 observations versus SWAN for the period of July 11–23, 2013, for (a) significant wave height (meters), (b) mean wave period (seconds), and (c) mean wave direction (degrees).

from the National Ocean Service (NOS, 2013). Surface current data for Cape Henry were obtained from NOS.

Model/Data Comparisons

Wind speeds were generally less than 10 m s^{-1} , primarily from the southwest-erly direction, during the periods of July 10–12 and July 18–22, with lower speeds and more variable directions during July 13–17. Figure 6 shows a model/data comparison at NDBC buoy 44099 for the period of July 10–24. Overall, the coupled system demonstrates very good skill. Observed wave heights were generally less than 1.1 m, with recorded minimums at or below 0.4 m on July 17–18. An overprediction of wave height by SWAN is evident during the peak events (e.g., July 13, 20, 21), which we attribute to poorly resolved features in the coarse resolution wind forcing. Wave directions are from the ESE throughout the period with wave periods generally between 4–6 s. Table 3 summarizes the wave statistics at the buoy with correlation coefficients ranging from 0.68 (wave direction) to 0.80 (period). RMSEs are generally within the accuracy of the measurements. The values shown in parentheses represent wave statistics without coupling to NCOM. Overall, the results show an improvement with coupling enabled.

Figure 7a shows a comparison of the observed water levels at the Chesapeake Bay Bridge-Tunnel (CBBV2-8638863) versus the elevations from NCOM, showing excellent agreement in phase with a small bias in the amplitude of -0.18 m . Table 4 (top) summarizes these results, which are highly correlated ($r = 0.96$). Surface currents from NCOM were examined at the Cape Henry NOS station (CB0102) indicated in Figure 6b,c. We found the u-component

Table 3. Observed versus modeled wave statistics at NDBC Buoy 44099 (Cape Henry). Values indicated in parentheses represent uncoupled results.

Buoy 44099	Bias	RMSE	r-statistic
Significant Wave Height (m)	0.13 (0.15)	0.19 (0.20)	0.78 (0.78)
Wave Period (s)	-0.30 (-0.29)	0.60 (0.60)	0.80 (0.77)
Wave Direction (°)	0.62 (-1.33)	11.7 (13.5)	0.71 (0.68)

Table 4. Observed versus modeled (NCOM) statistics for (top) water level at the Chesapeake Bay Bridge-Tunnel and (bottom) surface currents at Cape Henry (see Figure 3b for locations).

	Bias	RMSE	r-statistic
NOAA CBBV2-8638863			
Water Level (m)	-0.18	0.20	0.96
NOS CB0102			
Surface Current (m s^{-1})	0.19	0.16	0.33
U component	0.2547	0.1934	0.8465
V component	-0.0040	0.0424	0.5766

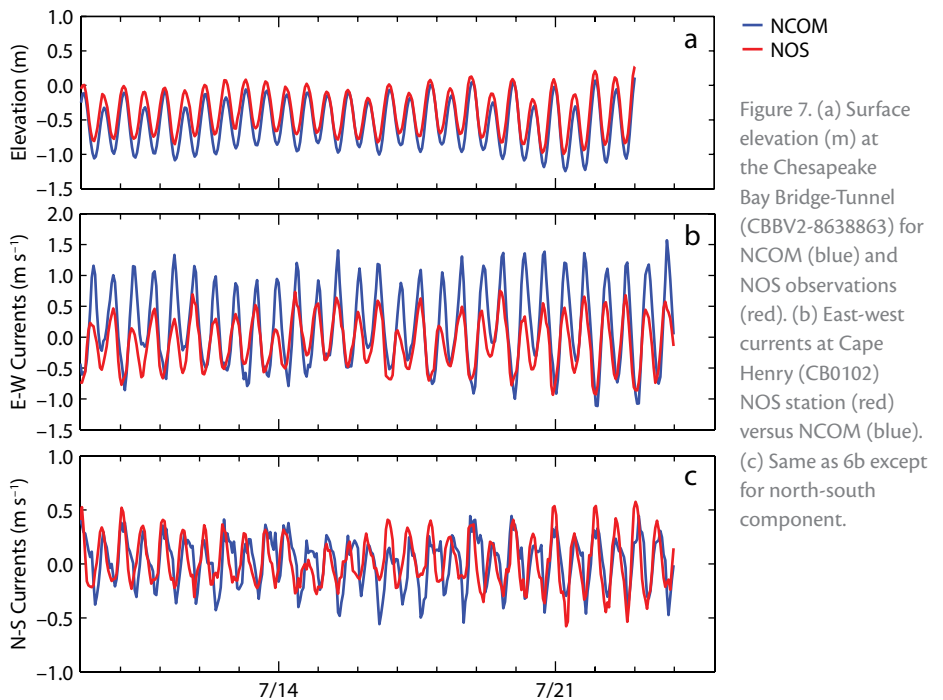


Figure 7. (a) Surface elevation (m) at the Chesapeake Bay Bridge-Tunnel (CBBV2-8638863) for NCOM (blue) and NOS observations (red). (b) East-west currents at Cape Henry (CB0102) NOS station (red) versus NCOM (blue). (c) Same as 6b except for north-south component.

in NCOM to be well correlated ($r = 0.85$), with a bias of 0.26 m s^{-1} and an RMSE of 0.19 m s^{-1} . The current's north-south component showed

reasonable agreement with NCOM, with a minimal bias and an RMSE of 0.04 m s^{-1} . However, there is an observed lag in NCOM of approximately 2 h.

FUTURE PLANS

Validation studies are being performed for the fully coupled, atmosphere-ocean-wave system in COAMPS, which is scheduled for operational implementation in late 2015. Test cases will include a broader area of study from Trident Warrior 2013 and the Dynamics of the Madden-Julian Oscillation (DYNAMO) CINDY field program that took place in the Indian Ocean in 2011. It is expected that the SWAN wave data assimilation system will be transitioned to operations in 2016. A new capability is being developed to couple COAMPS with the Los Alamos Community Ice Code (CICE) model. This new modeling system will facilitate high-resolution (1–3 km), regional, coupled, atmosphere-ocean-ice predictions for regions such as the Beaufort and Chukchi Seas.

ACKNOWLEDGEMENTS

The authors would like to thank Lucy Smedstad for providing access to global HYCOM boundary conditions for model testing, and David Sitton for and Brent Bartels for assistance with some of the figures and tables. This work was funded by the Office of Naval Research under program element 0602435N and by the Space and Naval Warfare Systems Command under program element 0603207N. This paper is NRL contribution number JA/7320–14–2007. 

COAMPS® is a registered trademark of the Naval Research Laboratory.

REFERENCES

- Allard, R.A., T.A. Smith, T.G. Jensen, P.Y. Chu, E. Rogers, T.J. Campbell, U.M. Gravois, S.N. Carroll, K. Watson, and S. Gaberšek. 2012. *Validation Test Report for the Coupled Ocean/Atmosphere Mesoscale Prediction System (COAMPS) Version 5.0: Ocean/Wave Component Validation*. NRL Memorandum Report NRL/MR/7320--12-9423, <http://www.dtic.mil/dtic/tr/fulltext/u2/a577284.pdf> (accessed March 27, 2014).
- Ardhuin, F., B. Chapron, and F. Collard. 2009. Observation of swell dissipation across oceans. *Geophysical Research Letters* 36, L06607, <http://dx.doi.org/10.1029/2008GL037030>.
- Ardhuin, F., E. Rogers, A. Babanin, J.-F. Filipot, R. Magne, A. Roland, A. van der Westhuysen, P. Queffelec, J.-M. Lefevre, L. Aouf, and F. Collard. 2010. Semi-empirical dissipation source functions for ocean waves. Part I: Definitions, calibration and validations. *Journal of Physical Oceanography* 40:1,917–1,941, <http://dx.doi.org/10.1175/2010JPO4324.1>.
- Asselin, R. 1972. Frequency filter for time integrations. *Monthly Weather Review* 100:487–490, [http://dx.doi.org/10.1175/1520-0493\(1972\)100<0487:FFFTI>2.3.CO;2](http://dx.doi.org/10.1175/1520-0493(1972)100<0487:FFFTI>2.3.CO;2).
- Babanin, A.V., K.N. Tsagareli, I.R. Young, and D.J. Walker. 2010. Numerical investigation of spectral evolution of wind waves. Part 2: Dissipation function and evolution tests. *Journal of Physical Oceanography* 40:667–683, <http://dx.doi.org/10.1175/2009JPO4370.1>.
- Banner, M.L., A.V. Babanin, and I.R. Young. 2000. Breaking probability for dominant waves on the sea surface. *Journal of Physical Oceanography* 30:3,145–3,160, [http://dx.doi.org/10.1175/1520-0485\(2000\)030<3145:BPFOWO>2.0.CO;2](http://dx.doi.org/10.1175/1520-0485(2000)030<3145:BPFOWO>2.0.CO;2).
- Barron, C.N., A.B. Kara, H.E. Hurlburt, C. Rowley, and L.F. Smedstad. 2004. Sea surface height predictions from the global Navy Coastal Ocean Model (NCOM) during 1998–2001. *Journal of Atmospheric and Oceanic Technology* 21:1,876–1,894, <http://dx.doi.org/10.1175/JTECH-1680.1>.
- Bleck, R. 2002. An oceanic general coordinate circulation model framed in hybrid isopycnic-Cartesian coordinates. *Ocean Modelling* 4:55–88, [http://dx.doi.org/10.1016/S1463-5003\(01\)00012-9](http://dx.doi.org/10.1016/S1463-5003(01)00012-9).
- Bennis, A.-C., F. Ardhuin, and F. Dumas. 2011. On the coupling of wave and three-dimensional circulation models: Choice of theoretical framework, practical implementation, and adiabatic tests. *Ocean Modelling* 40:260–272, <http://dx.doi.org/10.1016/j.ocemod.2011.09.003>.
- Blumberg, A.F., and G.L. Mellor. 1987. A description of a three-dimensional coastal ocean circulation model. Pp. 1–16 in *Three-Dimensional Coastal Ocean Models*. N. Heaps, ed., American Geophysical Union, New York, NY.
- Blumberg, A.F., and H. Herring. 1987. Circulation modelling using orthogonal curvilinear coordinates. Pp. 55–88 in *Three-Dimensional Models of Marine and Estuarine Dynamics*. J. Nihoul and B. Jamart, eds, Elsevier Oceanography Series, vol. 45.
- Booij, N., R.C. Ris, and L.H. Holthuijsen. 1999. A third-generation wave model for coastal regions: Part 1. Model description and validation. *Journal of Geophysical Research* 104(C4):7,649–7,666, <http://dx.doi.org/10.1029/98JC02622>.
- Bub, F.L., A.C. Mask, K.R. Wood, D.G. Krynen, B.N. Lunde, C.J. DeHaan, E.J. Metzger, P.G. Posey, and J.A. Wallmark. 2014. The Navy's application of ocean forecasting to decision support. *Oceanography* 27(3):126–137, <http://dx.doi.org/10.5670/oceanog.2014.74>.
- Campbell, T., R. Allard, R. Preller, L. Smedstad, A. Wallcraft, S. Chen, H. Jin, S. Gaberšek, R. Hodur, J. Reich, and others. 2010. Integrated modeling of the battlespace environment. *Computational Science and Engineering* 12(5):36–45, <http://dx.doi.org/10.1109/MCSE.2010.78>.
- Chen, S., T. Campbell, S. Gaberšek, R. Hodur, and P.J. Martin. 2010. Effect of two-way air–sea coupling in high and low wind speed regimes. *Monthly Weather Review* 138(9):3,579–3,602, <http://dx.doi.org/10.1175/2009MWR3119.1>.
- Cummings, J.A. 2005. Operational multivariate ocean data assimilation. *Quarterly Journal of the Royal Meteorology Society* 131:3,583–3,604, <http://dx.doi.org/10.1256/qj.05.105>.
- Davies, A.M., and J. Lawrence. 1994. Examining the influence of wind and wind-wave turbulence on tidal currents using a three-dimensional hydrodynamic model including wave-current interaction. *Journal of Physical Oceanography* 24:2,441–2,460, [http://dx.doi.org/10.1175/1520-0485\(1994\)024<2441:ETIOWA>2.0.CO;2](http://dx.doi.org/10.1175/1520-0485(1994)024<2441:ETIOWA>2.0.CO;2).
- Dietrich, D.E., and D.S. Ko. 1994. A semi-collocated ocean model based on the SOMS approach. *International Journal of Numerical Methods in Fluids* 19:1,103–1,113.
- Doyle, J.D. 2002. Coupled atmosphere–ocean wave simulations under high wind conditions. *Monthly Weather Review* 130:3,087–3,099, [http://dx.doi.org/10.1175/1520-0493\(2002\)130<3087:CAOWSU>2.0.CO;2](http://dx.doi.org/10.1175/1520-0493(2002)130<3087:CAOWSU>2.0.CO;2).
- Doyle, J.D., R.M. Hodur, S. Chen, Y. Jin, J.R. Moskaitis, S. Wang, E.A. Hendricks, H. Jin, and T.A. Smith. 2014. Tropical cyclone prediction using COAMPS-TC. *Oceanography* 27(3):104–115, <http://dx.doi.org/10.5670/oceanog.2014.72>.
- Donelan, M.A., A.V. Babanin, I.R. Young, and M.L. Banner. 2006. Wave follower field measurements of the wind input spectral function. Part II: Parameterization of the wind input. *Journal of Physical Oceanography* 36:1,672–1,688, <http://dx.doi.org/10.1175/JPO2933.1>.
- Dukhovskoy, D.S., S.L. Morey, P.J. Martin, J.J. O'Brien, and C. Cooper. 2009. Application of a vanishing, quasi-sigma, vertical coordinate for simulation of high-speed deep currents over the Sigsbee Escarpment in the Gulf of Mexico. *Ocean Modelling* 28:250–265, <http://dx.doi.org/10.1016/j.ocemod.2009.02.009>.
- Gravois, U., W.E. Rogers, and T.G. Jensen. 2012. *A Coupled Model System for Southeast Florida: Wave Model Validation Using Radar and In Situ Observations*. NRL Memorandum Report NRL/MR/7320--12-9355, 44 pp.

- Haney, R.L. 1991. On the pressure gradient force over steep topography in sigma coordinate ocean models. *Journal of Physical Oceanography* 21:610–619, [http://dx.doi.org/10.1175/1520-0485\(1991\)021<0610:OTPGFO>2.0.CO;2](http://dx.doi.org/10.1175/1520-0485(1991)021<0610:OTPGFO>2.0.CO;2).
- Haus, B.K. 2007. Surface current effects on the fetch limited growth of wave energy. *Journal of Geophysical Research* 112, C03003, <http://dx.doi.org/10.1029/2006JC003924>.
- Haus, B.K., P.A. Work, G. Voulgaris, N.K. Shay, R. Ramos, and J. Martinez. 2010. Wind speed dependence of single-site wave-height retrievals from high-frequency radars. *Journal of Atmospheric and Oceanic Technology* 27:1,381–1,394, <http://dx.doi.org/10.1175/2010JTECHO730.1>.
- Hodur, R.M. 1997. The Naval Research Laboratory's Coupled Ocean/Atmosphere Mesoscale Prediction System (COAMPS). *Monthly Weather Review* 125:1,414–1,430, [http://dx.doi.org/10.1175/1520-0493\(1997\)125<1414:TNRLSC>2.0.CO;2](http://dx.doi.org/10.1175/1520-0493(1997)125<1414:TNRLSC>2.0.CO;2).
- Holland, W.R., J.C. Chow, and F.O. Bryan. 1998. Application of a third-order upwind scheme in the NCAR ocean model. *Journal of Climate* 11:1,487–1,493, [http://dx.doi.org/10.1175/1520-0442\(1998\)011<1487:AOATOU>2.0.CO;2](http://dx.doi.org/10.1175/1520-0442(1998)011<1487:AOATOU>2.0.CO;2).
- Hogan, T.F., and T.E. Rosmond. 1991. The description of the Navy Operational Global Atmospheric Prediction System's spectral forecast models. *Monthly Weather Review* 119:1,786–1,815, [http://dx.doi.org/10.1175/1520-0493\(1991\)119<1786:TDOTNO>2.0.CO;2](http://dx.doi.org/10.1175/1520-0493(1991)119<1786:TDOTNO>2.0.CO;2).
- Hwang, P.A. 2011. A note on the ocean surface roughness spectrum. *Journal of Atmospheric and Oceanic Technology* 28:436–443, <http://dx.doi.org/10.1175/2010JTECHO812.1>.
- Kantha, L.H., and C.A. Clayson. 2004. On the effect of surface gravity waves on mixing in the oceanic mixed layer. *Ocean Modelling* 6:101–124, [http://dx.doi.org/10.1016/S1463-5003\(02\)00062-8](http://dx.doi.org/10.1016/S1463-5003(02)00062-8).
- Lesser, G., J.A. Roelink, J. van Kester, and G.S. Stelling. 2004. Development and validation of a three-dimensional morphological model. *Coastal Engineering* 51:883–915, <http://dx.doi.org/10.1016/j.coastaleng.2004.07.014>.
- Martin, P.J. 2000. *A Description of the Navy Coastal Ocean Model Version 1.0*. NRL Report NRL/FR/7322--00-9962, Naval Research Laboratory, SSC, MS 39529, 42 pp.
- Martin, P.J., E. Rogers, R.A. Allard, J.D. Dykes, and P.J. Hogan. 2013. *Tests of Parameterized Langmuir-Circulation Mixing in the Ocean's Surface Mixed Layer*. NRL Memorandum Report NRL/MR/7320--13-9444, 47pp.
- Mellor, G.L., and T. Yamada. 1974. A hierarchy of turbulence closure models for planetary boundary layers. *Journal of Atmospheric Science* 31:1,791–1,806, [http://dx.doi.org/10.1175/1520-0469\(1974\)031<1791:AHOTCM>2.0.CO;2](http://dx.doi.org/10.1175/1520-0469(1974)031<1791:AHOTCM>2.0.CO;2).
- Mellor, G.L., and P.A. Durbin. 1975. The structure and dynamics of the ocean surface mixed layer. *Journal of Physical Oceanography* 5:718–728, [http://dx.doi.org/10.1175/1520-0485\(1975\)005<0718:TSADOT>2.0.CO;2](http://dx.doi.org/10.1175/1520-0485(1975)005<0718:TSADOT>2.0.CO;2).
- Mellor, G.L., and T. Yamada. 1982. Development of a turbulence closure model for geophysical fluid problems. *Reviews of Geophysics* 20:851–875, <http://dx.doi.org/10.1029/RG020i004p00851>.
- Metzger, E.J., O.M. Smedstad, P.G. Thoppil, H.E. Hurlburt, J.A. Cummings, A.J. Wallcraft, L. Zamudio, D.S. Franklin, P.G. Posey, M.W. Phelps, and others. 2014. US Navy operational global ocean and Arctic ice prediction systems. *Oceanography* 27(3):32–43, <http://dx.doi.org/10.5670/oceanog.2014.66>.
- NOS (NOAA National Ocean Service). 2013. Tidal harmonics for Chesapeake Bay Bridge Tunnel, VA station ID: 8638863. <http://co-ops.nos.noaa.gov/waterlevels.html?id=8638863>.
- Phillips, O.M. 1958. The equilibrium range in the spectrum of wind generated waves. *Journal of Fluid Mechanics* 4:426–434, <http://dx.doi.org/10.1017/S0022112058000550>.
- Qiao, F., Y. Yuan, T. Ezer, C. Xia, Y. Yang, X. Lu, and Z. Song. 2010. A three-dimensional surface wave-ocean circulation coupled model and its initial testing. *Ocean Dynamics* 60:1,339–1,355, <http://dx.doi.org/10.1007/s10236-010-0326-y>.
- Rogers, W.E., A.V. Babanin, and D.W. Wang. 2012. Observation-consistent input and whitecapping-dissipation in a model for wind-generated surface waves: Description and simple calculations. *Journal of Atmospheric Oceanic Technology* 29(9):1,329–1,346, <http://dx.doi.org/10.1175/JTECH-D-11-00092.1>.
- Rowley, C., and A. Mask. 2014. Regional and coastal prediction with the Relocatable Ocean Nowcast/Forecast System. *Oceanography* 27(3):44–55, <http://dx.doi.org/10.5670/oceanog.2014.67>.
- Signell, R.P., R.C. Beardsley, H.C. Graber, and A. Capotondi. 1990. Effect of wave-current interaction on wind-driven circulation in narrow, shallow embayments. *Journal of Geophysical Research* 95(C6):9,671–9,678, <http://dx.doi.org/10.1029/JC095iC06p09671>.
- Singhal, G., V.G. Panchang, and J.A. Nelson. 2013. Sensitivity assessment of wave heights to surface forcing in Cook Inlet, Alaska. *Continental Shelf Research* 63:S50–S62, <http://dx.doi.org/10.1016/j.csr.2012.02.007>.
- Smagorinsky, J. 1963. General circulation experiments with the primitive equations: I. The basic experiment. *Monthly Weather Review* 91:99–164, [http://dx.doi.org/10.1175/1520-0493\(1963\)091<0099:GCEWTP>2.3.CO;2](http://dx.doi.org/10.1175/1520-0493(1963)091<0099:GCEWTP>2.3.CO;2).
- Smith, T.A., S. Chen, T. Campbell, P. Martin, W.E. Rogers, S. Gaberšek, D. Wang, S. Carroll, and R. Allard. 2013. Ocean-wave coupled modeling in COAMPS-TC: A study of Hurricane Ivan (2004). *Ocean Modelling* 69:181–194, <http://dx.doi.org/10.1016/j.ocemod.2013.06.003>.
- Tang, C.L., W. Perrie, A.D. Jenkins, B.M. DeTracey, Y. Hu, B. Toulany, and P.C. Smith. 2007. Observation and modeling of surface currents on the Grand Banks: A study of the wave effects on surface currents. *Journal of Geophysical Research* 112, C10025, <http://dx.doi.org/10.1029/2006JC004028>.
- Taylor, L.A., B.W. Eakins, K.S. Carignan, R.R. Warnken, T. Sazonova, D.C. Schoolcraft, and G.F. Sharman. 2008. *Digital Elevation Model of Virginia Beach, Virginia: Procedures, Data Sources and Analysis*. NOAA Technical Memorandum NESDIS NGDC-7, National Geophysical Data Center, Boulder, CO, 34 pp.
- Tolman, H.L. 2009. *User Manual and System Documentation of WAVEWATCH III/TM Version 3.14*. Technical Note, NOAA/NWS/NCEP/MMAB, 220 pp.
- SWAN Team. 2010. *SWAN Scientific and Technical Documentation, SWAN Cycle III Version 40.81*. Delft University of Technology, 118 pp. See: <http://www.swan.tudelft.nl>.
- Tsagareli, K.N. 2009. Numerical investigation of wind input and spectral dissipation in evolution of wind waves. PhD Thesis, University of Adelaide, Australia, 217 pp.
- Tsagareli, K.N., A.V. Babanin, D.J. Walker, and I.R. Young. 2010. Numerical investigation of spectral evolution of wind waves. Part 1: Wind input source function. *Journal of Physical Oceanography* 40:656–666, <http://dx.doi.org/10.1175/2009JPO4345.1>.
- Veeramony, J., M.D. Orzech, K.L. Edwards, M. Gilligan, J. Choi, E. Terrill, and T. De Paolo. 2014. Navy nearshore ocean prediction systems. *Oceanography* 27(3):80–91, <http://dx.doi.org/10.5670/oceanog.2014.70>.
- Voulgaris, G., B.K. Haus, P. Work, L.K. Shay, H. Seim, R.H. Weisberg, and J.R. Nelson. 2008. Waves initiative within SEACOOS. *Marine Technology Society Journal* 42(3):68–80.
- Warner, J.C., C.R. Sherwood, R.P. Signell, C.K. Harris, and H.G. Arango. 2008. Development of a three-dimensional, regional, coupled wave, current, and sediment transport model. *Computers & Geosciences* 34:1,284–1,306, <http://dx.doi.org/10.1016/j.cageo.2008.02.012>.
- White, J. 2014. Challenges and opportunities: Naval oceanography in 2013. *Sea Technology* 55(1):16–18, http://www.sea-technology.com/features/2014/0114/4_White.php.
- Young, I.R., and A.V. Babanin. 2006. Spectral distribution of energy dissipation of wind-generated waves due to dominant wave breaking. *Journal of Physical Oceanography* 36:376–394, <http://dx.doi.org/10.1175/JPO2859.1>.
- Zalesak, S.T. 1979. Fully multidimensional flux-corrected transport algorithms for fluid. *Journal of Computational Physics* 31:335–362, [http://dx.doi.org/10.1016/0021-9991\(79\)90051-2](http://dx.doi.org/10.1016/0021-9991(79)90051-2).